JOURNAL OF SOLID STATE CHEMISTRY **133,** 169–177 (1997)
ARTICLE NO. SC977334

Some Chemical and Physical Properties of Quaternary Borocarbides

C. Godart, E. Alleno, and E. Tominez

CNRS, LCMSTR, UPR 209, 92195 Meudon Cedex, France

L. C. Gupta, R. Nagarajan, and Z. Hossain

TIFR, 400001 Bombay, India

J. W. Lynn

NIST, Gaithersburg, Maryland 20899

P. Bonville and J. A. Hodges

CEA, 91191 Gif sur Yvette, France

J. P. Sanchez

CEA, 38054 Grenoble, France

and

I. Felner

University of Jerusalem, Israel

Received January 30, 1997; accepted February 12, 1997

The recent discovery of superconductivity (SC) in the quaternary borocarbide system Y–Ni–B–C has opened up a new area of research in SC. SC mainly occurs only for the end members of rare earths (*R*) and magnetism and SC coexist when *R* is a magnetic ion (Ho, Er, Tm, and later in Dy). We will discuss and give some new results on the effects of annealing on the impurity phases and on low Fe doping rates on the coexistence between SC and magnetism in materials with *R* = Ho. Superconductivity has been reported in Y–Pd–B–C system with a T_c (22 to 23 K) higher than the record for bulk intermetallics. The composition and structure of the SC phase(s) is still a topic of controversy that we will briefly discuss, giving new results.

INTRODUCTION

The recent discovery of superconductivity (SC) in the quaternary borocarbide system Y–Ni–B–C (1, 2) has opened up a new area of research in SC. Superconductivity was reported in single phase materials RNi_2B_2C (3) (R = rare earths, Y) having a tetragonal structure (I4/mmm) (4). The remarkable properties of these materials have generated a very large activity during the past 3 years (5). SC mainly occurs only for the end members of R elements and magnetism and SC coexist when R is a magnetic ion (Ho, Er, Tm, and later in Dy) (6–10). The most striking feature of these magnetic superconductors (MSC), which distinguishes them from all other MSC, is their high magnetic transition temperatures which are of the order of their SC temperatures T_c. We will discuss and give some new results on the effect of annealing temperatures on the existence of the impurity phase RB_2C_2 (R = Ho, Er, Tm) and on the coexistence between SC and magnetism in Ho-based materials in the case of low Fe doping. The starting members of R elements do not superconduct and many of them are only magnetic (11). Surprisingly, SC does not appear in $YbNi_2B_2C$ down to 2 K even though Yb is close to be trivalent. This may be related to moderately heavy fermion behavior (10, 12). $CeNi_2B_2C$ has been reported as a non-SC intermediate valence compound (13, 14). Superconductivity has been reported in Y–Pd–B–C system (15, 16) with a T_c (22 to 23 K) higher than the record for bulk intermetallics. The composition and structure of the SC phase(s) is still a topic of controversy that we will briefly discuss, giving new results. SC has also been found in Sc–Ni (17) and Th–Ni-and Th–Pd-based (18, 19), as well as in some Pt-based (20–24)

0022-4596/97 $25.00

quaternary borocarbides. New borocarbides $R\mathrm{Ni}_{1-x}\mathrm{Cu}_x\mathrm{BC}$ (R = Y, Lu) having T_c up to 8.9 K (25), claim (not confirmed by other groups) for SC up to 16 K in $R\mathrm{Ni}_4\mathrm{B}_4\mathrm{C}$ (26), and new boronitrides $R_3\mathrm{Ni}_2\mathrm{B}_2\mathrm{N}_3$ (27, 28) with T_c up to 12 K, in Ni-based materials, give a pretty unique character to this family of quaternary materials.

$R\mathrm{Ni}_2\mathrm{B}_2\mathrm{C}$ SYSTEMS

We and other authors have discussed competition or coexistence of superconductivity and magnetism (or hybridization effects) in quaternary borocarbides through many papers. As we go through the literature on this topic, it is surprising to observe that the "same" material has different properties and it is only in very rare cases that its nominal composition is mentioned. We agree that some of the experiments to chemically characterize samples are meaningless due to the presence in the material of two light elements (B and C)—see below, under Y–Pd–B–C, a brief discussion on this peculiar point. However, initial composition, values of lattice parameters (of ~ 250 papers, we find ~ 65 values of lattice parameters), and temperatures of annealing are not given often enough and the loss of information on the effects on the physical properties is enormous. An interesting study which has been performed in the case of 1100°C-annealed $\mathrm{HoNi}_2\mathrm{B}_2\mathrm{C}$ samples shows the nonstoichiometry and phases in equilibrium to be correlated with the existence of superconductivity, reentrance of the SC or non-SC (29). Nonstoichiometry effects have also been studied in $\mathrm{DyNi}_2\mathrm{B}_2\mathrm{C}$ and correlated with the existence of SC or not (8). Let us recall that a time interval of about 1 year separates the discovery of SC in $R\mathrm{Ni}_2\mathrm{B}_2\mathrm{C}$ with that of SC in Dy-based material, probably due to its very unique property of having T_{mag} (11 K) higher than T_c (6 K), which means that SC has to develop in an already ordered magnetic lattice.

We emphasize the importance of chemistry in this series from different aspects. First of all, compiling the values of the lattice parameters already published, we draw Fig. 1 for the various R elements in $R\mathrm{Ni}_2\mathrm{B}_2\mathrm{C}$. In that figure, the size of the symbols corresponds to an error bar of $\pm 1\%$, a value easily obtained from standard X ray diffraction (XRD) experiments (about 0.003 Å on the a parameter and about 0.01Å on the c-parameter). We do remark that the dispersion of points is always larger than these error bars. This indicates that a domain of existence exists for more or less all the materials of the series, and this is in agreement with the variety of physical properties observed in many individual cases. However, this point has never been mentioned.

Concerning annealing effects, it has been mentioned by (30) that $\mathrm{YNi}_2\mathrm{B}_2\mathrm{C}$ should be annealed above 1050°C, even though adhesion often occurs to the Ta or Mo foil used to encapsulate the sample and protect it from the quartz tube.

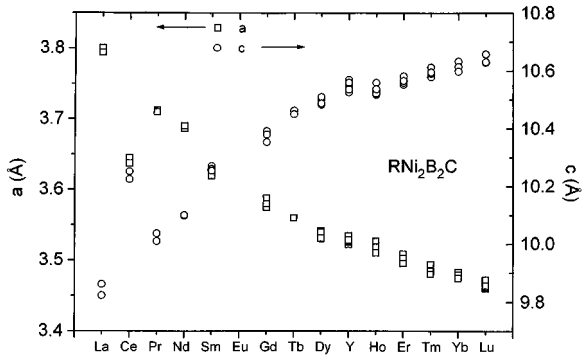

FIG. 1. Lattice parameters (Å) a (left scale) and c (right scale) in $R\mathrm{Ni}_2\mathrm{B}_2\mathrm{C}$ (R = rare earths, Y), the size of the symbols corresponds to an error bar of $\pm 1\%$.

However, at such a temperature some oxidation will also take place (from the quartz tube) and that may be the reason why their sample has a T_c of 14.2 K compared to ~ 15.3 K. Nevertheless, annealing effects on the physical properties is very well illustrated by the case of the reentrance to SC in $\mathrm{HoNi}_2\mathrm{B}_2\mathrm{C}$ (see, for instance, Fig. 2 of (31)). We report here a similar effect in ^{57}Fe-doped $\mathrm{HoNi}_2\mathrm{B}_2\mathrm{C}$ (see Fig. 2) in which the unannealed sample shows only a slight decrease of the resistivity at 7 K, with a slight indication of reentrance at 5 K, whereas the two phenomena are an order of magnitude larger on the same sample annealed at 800°C for 2 weeks. This annealing temperature seems close to optimal as we observe that one of the main impurities first identified is $R\mathrm{B}_2\mathrm{C}_2$ (32) (magnetic properties (33, 34) of $R\mathrm{B}_2\mathrm{C}_2$ can be detrimental to SC) essentially disappears when $\mathrm{HoNi}_2\mathrm{B}_2\mathrm{C}$ is annealed 2 weeks at 700°C, but reappears at higher temperature (800°C) and grows up at 900°C (Fig. 3). In the case of $\mathrm{GdNi}_2\mathrm{B}_2\mathrm{C}$, $\mathrm{GdB}_2\mathrm{C}_2$ disappears when annealed at 900°C for 2 weeks (see Fig. 4). In $\mathrm{TmNi}_2\mathrm{B}_2\mathrm{C}$, annealing at 800°C lowers the $\mathrm{TmB}_2\mathrm{C}_2$ impurity content more than at 900°C (35). On the other hand, $\mathrm{CeNi}_2\mathrm{B}_2\mathrm{C}$ needs to be annealed at 1050°C to obtain a single phase material, but we used shorter period (4 days) in order to avoid a deep oxidation (14). We should then notice that the equilibrium $R\mathrm{Ni}_2\mathrm{B}_2\mathrm{C}$ and $R\mathrm{B}_2\mathrm{C}_2$ apparently does not occur in the same way along the R-series and conclude that the annealing temperatures for $R\mathrm{Ni}_2\mathrm{B}_2\mathrm{C}$ should be progressively reduced from the starting toward the end members of the R-elements.

Of course, impurities may also play an important role as substitution effects are very efficient in decreasing T_c, particularly substitutions on the Ni site as the Ni–B sublattice is assumed to play a major role in SC (see for instance, (36–40)). Such substitutions have been performed at a rather high level, typically 5–10%, but the effect of a low level of substitution (however, a large value for an elemental impurity content) is illustrated by the resistivity curves (Fig. 2)

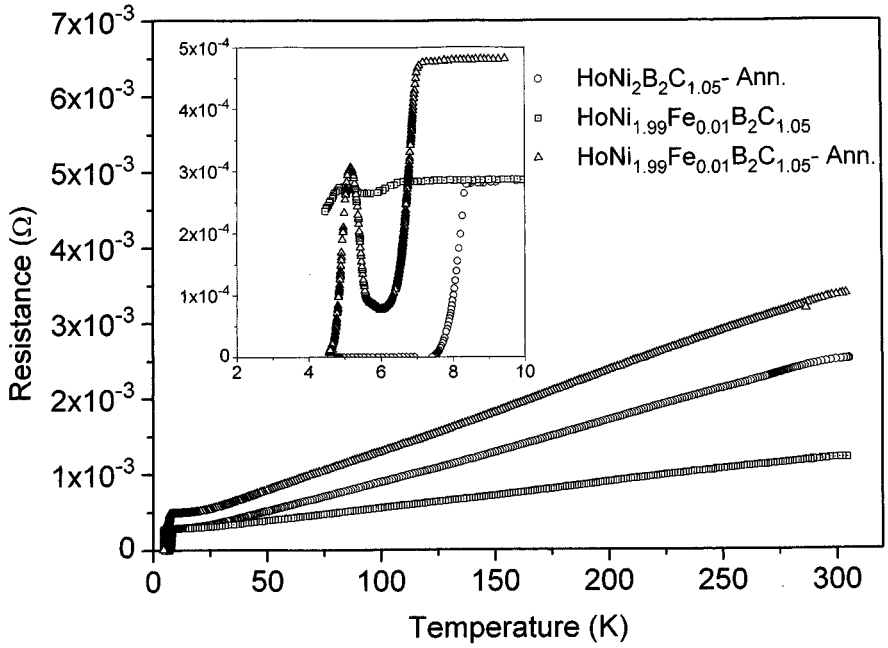

FIG. 2. Resistance (Ω) versus temperature in $HoNi_2B_2C_{1.05}$-annealed and $HoNi_{1.99}Fe_{0.01}B_2C_{1.05}$-unannealed and -annealed.

obtained on annealed samples of undoped and half percent ^{57}Fe-doped $HoNi_2B_2C_{1.05}$. The undoped sample becomes a superconductor at 8 K, whereas the Fe-doped one shows SC at a lower T_c (7.1 K) and reentrance at 5 K.

Y–Pd–B–C SYSTEM

With respect to high T_cs, the quaternary based system (Y–Pd–B–C) has led to the finding of a high T_c (23 K) (15) in a sample of nominal composition $YPd_5B_3C_x$ ($0.3 \leq x \leq 0.5$), the strongest superconducting signal being observed with $x \sim 0.35$. Many authors do find superconductivity around 22 K (22 K-phase) with other nominal compositions: $YPd_4B_1C_x$ ($0.2 \leq x \leq 1$) (7, 16), $YPd_4B_4C_y$ ($y < 0.1$) and $YPd_3B_2C_z$ ($z < 0.1$) (41), $YPd_2B_2C_w$ (42). We should note that all these materials are multiphase from XRD analysis. In all these materials, annealing in the range 800–900°C destroys superconductivity, but samples stay multiphase

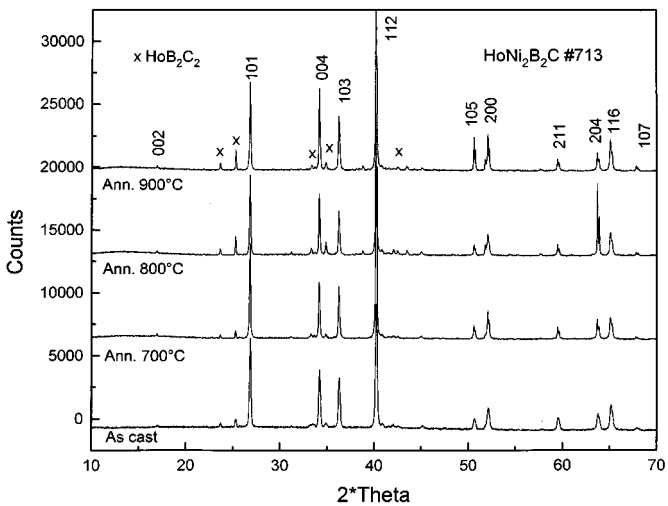

FIG. 3. X ray diffraction spectra in $HoNi_2B_2C$, as-cast and annealed at 700, 800, and 900°C. Symbol × indicates main peaks of HoB_2C_2.

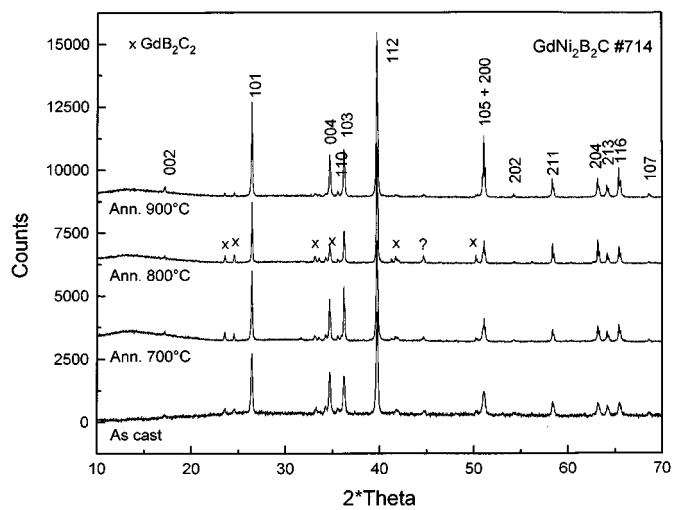

FIG. 4. X ray diffraction spectra in $GdNi_2B_2C$, as-cast and annealed at 700, 800, and 900°C. Symbol × indicates main peaks of GdB_2C_2.

and no definite conclusion can be drawn from the analysis of XRD patterns. Another superconducting phase has been reported with T_c around 10 K (10 K-phase) in $YPd_4B_1C_x$ ($0.2 \leq x \leq 1$) (7, 16), as well as in Lu (7, 16) and Th (18)-based similar compositions. From these results, it appears that *at least two superconducting phases* exist in the systems. The identification of the superconducting phases has led to a large number of propositions for the possible structure of the 22–23 K Y–Pd–B–C–based superconducting phase. Chemical analysis cannot be used, as only a fraction of the multiphase sample belongs to the SC phase. Further, the technique is not sensitive enough to determine quantitatively the elemental concentrations when there are two light elements, like B and C, in the materials. Intensity calculation and/or Rietveld analysis also does not work for the same reasons. TEM (Transmission Electron Microscope) and electron microprobe are more or less insensitive to light elements like B and C. From high resolution electron microscopy (HREM), it was proposed (43–45) that a centered tetragonal phase with $a \sim 37$–3.8 Å and $c \sim 10.6$–10.8 Å is the right superconducting phase, that phase could be some non stoichiometric "$YPd_2B_{2-x}C$." However, we point out that B and C have a very small effect on image contrast and that Y and Pd have similar scattering factors and consequently are not really distinguishable. A ternary cubic phase, possibly $YPd_{1.2}B_{3.3}$ also exists and disappears when $T_c \sim 23$ K disappears (46). According to (47) this "YPd_2B_2C" is metastable and cannot be stabilized by Ni substitution. Rapidly quenched sample of nominal composition YPd_2B_2C (48, 49) was found superconducting at 21 K (the as-cast sample does not superconduct) for a cubic phase (fcc with $a = 4.15$ Å). When annealed, this cubic phase disappears, as does superconductivity. Unfortunately, the authors do not discuss eventual changes of the a parameter during this process, but they mention that this cubic phase does not exist in superconducting quenched YPd_3B_3C and as-cast or quenched $YPd_5B_3C_{0.35}$. Let us note that in Th–Pd–B–C also, two superconducting phases have been reported ($T_{c1} \sim 14$–15 K and $T_{c2} \sim 19$–20 K) (18, 19) and that both quaternary tetragonal (19, 46, 50) and ternary cubic phases (46) have been found from HREM and are supposed to be responsible for superconductivity. The cubic phase (primitive, $a = 4.2$ Å) could be $ThPd_{0.65}B_{4.7}$ (probably CaB_6-type), and it may be responsible for $T_{c1} \sim 21$ K.

In order to improve the knowledge of the phase diagram and look for other compositions, close to those of previous quaternaries that could be responsible for superconductivity, we prepared and studied $YPd_2B_{1+x}C$ ($x = 0$, 0.2, 0.4, 0.5, 0.6, 0.8, and 1) to check nonstoichiometry effects, $Y_3Pd_{13}B_mC_1$ ($m = 2$, 3, 5, 7, and 8) and $Y_3Pd_{13-p}B_2C$ ($p = 0$, 1, and 2), as $Y_3Ni_{13}B_2$ forms in an hexagonal structure. From XRD examination, all these samples are multiphase, except $Y_3Pd_{13}B_2C_1$, in which a cubic phase (see Fig. 5) with $a = 4.098$ Å has been observed with only minor impurity phases. This result was confirmed by Cu-Guinier camera measurements which show a major phase, probably YPd_3B, when compared with $PrPd_3B$, and a minor Pd_3B phase. Metallographic examination shows a major phase and a minor one and electron microprobe analysis of Y and Pd (B and C cannot be measured) reveals a ratio Y/Pd for the major phase between 1/3 to 1/4, which indicates that the phase may be B-deficient as compared to YPd_3B. Let us note that in the binary Y–Pd system, YPd_3, forms and probably YPd_4 also does (as $ThPd_4$ is known), both with the $AuCu_3$ structure type. In the $AuCu_3$ structure, a large capability for atomic exchange exists as the site 1a is filled with 20%Pd and 80%Th and consequently should accept B atoms. This cubic phase progressively disappears in $Y_3Pd_{13}B_mC_1$ when m increases and XRD analysis shows that extra phases are growing. Unfortunately, $Y_3Pd_{13}B_2C_1$ does not show superconductivity, which appears (see Table 1) only in $Y_3Pd_{13}B_mC_1$ with $m \geq 7$ in a sample containing a large number of phases. In the series $YPd_2B_{1+x}C$, XRD shows a cubic phase with $a \sim 4.1$ Å (see Fig. 6) which is the major phase when $x = 0$ and undergoes a rhombohedral distortion when x increases and finally disappears for x higher than 0.5. On the other hand, a tetragonal minor phase already visible when $x = 0$ increases with x. Weak superconducting signals ($\leq 1\%$ Meissner effect) are observed in every sample (see Fig. 7), except in YPd_2B_2C. However, let us notice that the very weak superconducting signal cannot be attributed to either the cubic or the tetragonal phases as their observed XRD intensities represent more than 1% of the intensity of the main line. Our results about this cubic phase (or phases) disagree with those of (48, 49), implying that superconductivity is related to a metastable phase closely correlated to a fcc structure. In YPd_2B_1C (low B concentration) superconductivity exists only at 10 K, whereas other samples show both superconducting phases around 10 and 22 K (see Table 1). Annealing at 500°C for 3 weeks $YPd_2B_{1.2}C$ does not destroy

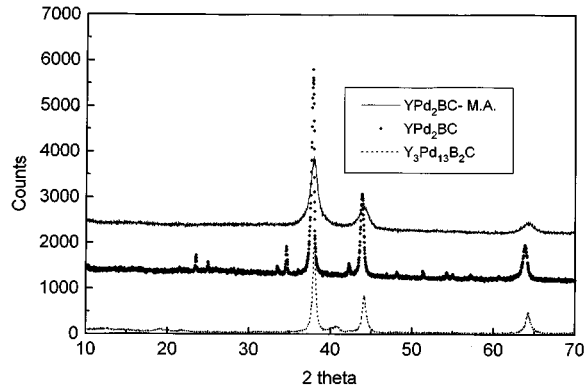

FIG. 5. X ray diffraction spectra in YPd_2BC. M.A. (mechanical alloying), YPd_2BC and $Y_3Pd_{13}B_2C$ (as-cast, arc furnace).

TABLE 1
Superconducting and Nonsuperconducting (NS) Y–Pd–B–C

Y	Pd	B	C	Y_{nor}	Pd_{nor}	B_{nor}	C_{nor}	Sup.	Ref.
1	5	3	0.5	10.53	52.63	31.58	5.26	23	42
1	5	3	0.4	10.64	53.19	31.91	4.26	23	15
1	5	3	0.35	10.70	53.48	32.09	3.74	23	15, 49
1	5	3	0.3	10.75	53.76	32.26	3.23	23	45, 47
1	4	4	0.1	10.99	43.96	43.96	1.10	23	41
1	4.2	3	0.3	11.76	49.41	35.29	3.53	23	47
3	13	8	1	12	52	32	4	22	This work
1.25	4.5	4.25	0.1	12.38	44.55	42.08	0.99	23	15
3	13	7	1	12.5	54.17	29.17	4.17	22	This work
1	3	3	0.3	13.70	41.10	41.10	4.11	22	47
1	4	1	1	14.29	57.14	14.29	14.29	22	16
1.5	4.5	4	0	15	45	40	0	23	15
1	4	1	0.5	15.38	61.54	15.38	7.69	22	36, 16
1	4	1	0.5	15.38	61.54	15.38	7.69	10	36, 16
1	4	1	0.2	16.13	64.52	16.13	3.23	22	36, 16
1	3	2	0.1	16.39	49.18	32.79	1.64	22	41
1	2	1.8	1	17.24	34.48	31.03	17.24	10	This work
1	2	1.8	1	17.24	34.48	31.03	17.24	22	This work
1	2	1.5	1.2	17.54	35.09	26.32	21.05	10	This work
1	2	1.5	1.2	17.54	35.09	26.32	21.05	22	This work
1	2	1.6	1	17.86	35.71	28.57	17.86	10	This work
1	2	1.6	1	17.86	35.71	28.57	17.86	22	This work
1	2	1.5	1	18.18	36.36	27.27	18.18	10	This work
1	2	1.5	1	18.18	36.36	27.27	18.18	22	This work
1	2	1.4	1	18.52	37.03	25.93	18.52	22	This work
1	2	1.2	1	19.23	38.46	23.08	19.23	10	This work
1	2	1.2	1	19.23	38.46	23.08	19.23	22	This work
1	2	1	1	20	40	20	20	10	This work
1	2	2	0	20	40	40	0	20	49
1	1	1	1	25	25	25	25	9.5	49
1	1	1	1	25	25	25	25	9	This work
1	7	4	1	7.69	53.85	30.77	7.69	NS	47
1	3	8	0.1	8.26	24.79	66.12	0.83	NS	41
1	7	4	0.1	8.26	57.85	33.06	0.83	NS	47
1	6	4	1	8.33	50	33.33	8.33	NS	This work
1	6	3	1	9.09	54.55	27.27	9.09	NS	This work
1	4	4	1	10	40	40	10	NS	49
1	5	3	1	10	50	30	10	NS	42
1	5	3	0.5	10.53	52.63	31.58	5.26	NS	15
1	5	3	0.2	10.87	54.35	32.61	2.17	NS	15
1	4	4	0.1	10.99	43.96	43.96	1.10	NS	41
1	5	3	0.1	10.99	54.95	32.97	1.10	NS	42
1	4	3.6	0.4	11.11	44.44	40	4.44	NS	This work
1	3	4	0.1	12.35	37.04	49.38	1.23	NS	41
3	13	5	1	13.64	59.09	22.73	4.55	NS	This work
1	3	3	0.2	13.89	41.67	41.67	2.78	NS	47
1	2	3.6	0.2	14.71	29.41	52.94	2.94	NS	This work
3	13	3	1	15	65	15	5	NS	This work
1	2	3	0.5	15.38	30.77	46.15	7.69	NS	This work
3	13	2	1	15.79	68.42	10.53	5.26	NS	This work
1	2	2.2	1	16.13	32.26	35.48	16.13	NS	This work
1	1	4	0.1	16.39	16.39	65.57	1.64	NS	41
1	1	3	1	16.67	16.67	50	16.67	NS	47
1	2	2	1	16.67	33.33	33.33	16.67	NS	This work
1	3	2	0	16.67	50	33.33	0	NS	41
3	12	2	1	16.67	66.67	11.11	5.56	NS	This work
1	4	1	0	16.67	66.67	16.67	0	NS	7
1	4	1	0	16.67	66.67	16.67	0	NS	16
3	11	2	1	17.65	64.71	11.76	5.88	NS	This work
1	2	2	0.1	19.61	39.22	39.22	1.96	NS	41
1	3	1	0.1	19.61	58.82	19.61	1.96	NS	41
1	2	1.5	0	22.22	44.44	33.33	0	NS	This work
1	1	2	0.1	24.39	24.39	48.78	2.44	NS	41

Note. Initial compositions, columns 1–4; compositions normalized to 100, columns 5–8.

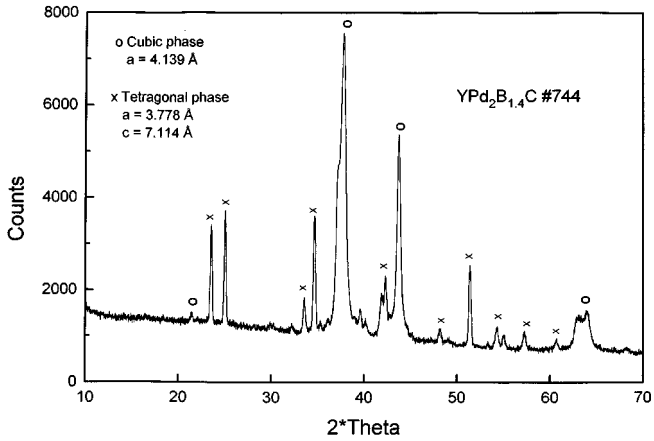

FIG. 6. X ray diffraction spectra in $YPd_2B_{1.4}C$ showing a cubic phase (○) and a tetragonal phase (×). Within the size of the figure, rhombohedral distortion can be seen easily on the left side of the main peak.

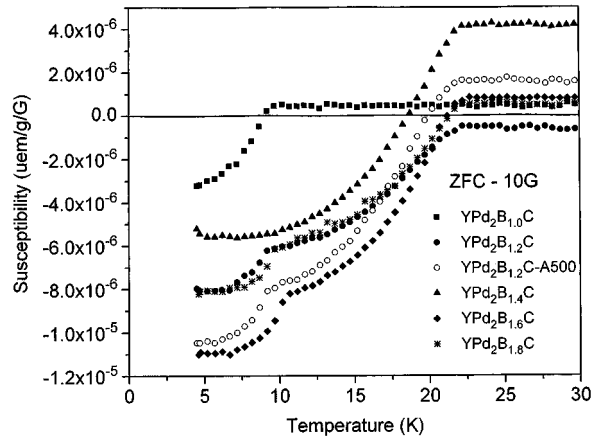

FIG. 7. Magnetic susceptibility (zero field cooled, ZFC) measured with 10 G, versus temperature in $YPd_2B_{1+x}C$ unannealed. Results for $YPd_2B_{1.2}C$ annealed at 500°C are also shown.

superconductivity at 10 and 22 K but annealing at 800°C does. In order to study the role of amorphization, mechanical alloying has been used to prepare YPd_2BC (see Fig. 5). Superconductivity has not been observed in the as-prepared and in the annealed sample. Conversely, YNi_2B_2C prepared by mechanical alloying does not show superconductivity when as-prepared, but superconductivity appears after annealing at 800°C for 3 days. $Y_3Pd_{13-p}B_2C$ ($p = 0$, 1, and 2) does not show superconductivity.

We compile in Table 1 nominal compositions and superconducting or non superconducting properties from data in the literature with our new results. Now, we will show how it is possible to establish correlations between the SC properties of a sample and its nominal composition by plotting a quaternary phase diagram. Some authors tried to find correlations in a pseudoternary phase diagram keeping a constant concentration for one of the elements. However, this is a crude approximation. For example, two quaternary compounds of close compositions, $A_1B_2C_2D_1$ and $A_1B_2C_2D_{1.1}$, can also be respectively represented by $A_{16.67}B_{33.33}C_{33.33}D_{16.67}$ and $A_{16.39}B_{32.79}C_{32.79}D_{18.03}$ and they obviously cannot belong to the same pseudoternary phase diagram. To our knowledge, representation of a quaternary phase diagram has not been reported, so let us make some comments. A quaternary phase diagram can be represented in a regular tetrahedron with each corner corresponding to a pure element. The rules for plotting a compound in this tetrahedron are of course similar to the rules for ternary phase diagrams. A line starting from the element A and joining a point on the line B–C, in ternary diagram, which corresponds to constant ratio of B/C elements along the line will be replaced, in quaternary diagram, by a plane starting from A and B and joining a point on the line C–D (for instance) and will be the plane of constant C/D ratio. This plane will separate two regions, each corresponding to compositions richer in C or in D than the constant C/D ratio. A compound of fixed composition defines six planes of constant ratio between two given elements. We choose a "1221" composition as it seems to be a good reference, using *R*–*M*–B–C (*R* for rare earth, *M* for d metal, *B* for boron, and C for carbon) notation. On Figs. 8a to 8f, we present 6 projections of a reduced tetrahedron made of four triangular planes corresponding to 10% of *R*, *M*, B, and C, respectively. The use of this reduced tetrahedron leads to an increased view of the part of the diagram of interest. On these figures, the six planes of constant ratio (corresponding to "1221") are in each case set perpendicular to the sheet of paper and appear only by their trace (shown by a thick line). For convenience, we also rotate the projections so that the axis between the two elements which define the ratio appears horizontal. A plane noted *RM*(BC), for instance, is a plane of constant B/C ratio passing by *R* and *M*. Consequently, the right and left sides of this plane will correspond to richer or poorer compositions than B/C = 2/1. It is necessary to use the six projections to be sensitive to the various ratio *R*/*M*, *R*/B, *R*/C, *M*/B, *M*/C, and B/C, as on one figure (paper sheet being two-dimensional) the third dimension will not appear.

FIG. 8. (a) Projection of quaternary phase diagram. *R*, *M*, B, and C correspond to reduced tetrahedra (see text), showing the trace of the plane *RM*(BC) (thick line) and nonsuperconducting (SUP) (□), 22 K SUP (●), and 10 K SUP (▨) nominal compositions in Y–Pd–B–C system. (b) Trace of the plane *R*C(*M*B) (thick line), (c) trace of the plane *R*B(C*M*) (thick line), (d) trace of the plane *MC*(*R*B) (thick line), (e) trace of the plane CB(*RM*) (thick line), (f) trace of the plane *M*B(*R*C) (thick line).

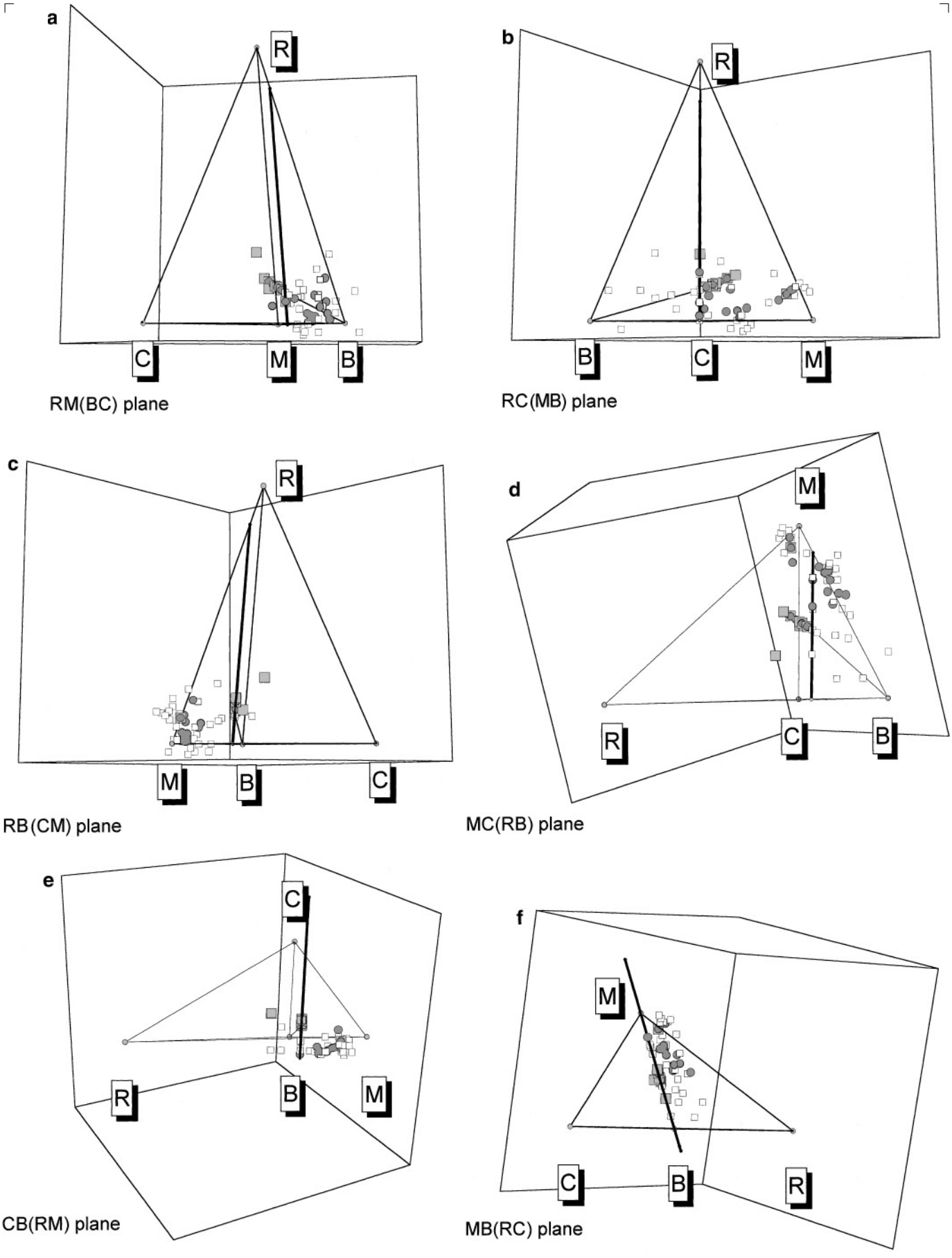
a
R
C
M
B
RM(BC) plane
b
R
B
C
M
RC(MB) plane
c
R
M
B
C
RB(CM) plane
d
M
R
C
B
MC(RB) plane
e
C
R
B
M
CB(RM) plane
f
M
C
B
R
MB(RC) plane

We also plotted on these six projections the available data (Table 1) on the Y–Pd–B–C for arc melted samples with open squares when non-SC, full square when SC at 10 K exists and full circle when SC at 22–23 K. In Fig. 8a, for the plane RM(BC), the 10 K phase (large full square) appears on the C-rich side relative to the composition B_2C_1, whereas the 22 K phase (full circle) appears on both sides. In Fig. 8b, for the plane RC(MB), the 10 K phase and the 22 K phase appear both on the M-rich side relative to M_2B_2. In Fig. 8c, for the plane RB(CM), the 22 K phase appears on the M-rich side relative to M_2C_1. In Fig. 8d, for the plane MC(RB), the 10K phase appears on the R-rich side relative to R_1B_2. In Fig. 8e, for the plane CB(RM), the 22 K phase appears on the M-rich side relative to R_1M_2. In Fig. 8f, for the plane MB(RC), the 22 K phase appears on the R-rich side relative to R_1C_1, whereas the 10 K phase is roughly on the plane R_1C_1. From Figs. 8a, 8c, 8d, 8e, and 8f, it appears that there is a clear separation between the domains in which the 10 K and the 22 K phase appears. This seems to indicate that the 10 K phase and the 22 K phase have different compositions. Chemical analysis of the phases in equilibrium would be necessary to improve the knowledge of the phase diagram. However, these efforts would be greatly restricted due to the above-mentioned difficulties in performing such measurements.

ACKNOWLEDGMENTS

We thank Dr. M. Vybornov for Guinier camera measurements and useful discussions on structures. We thank M. L. Touron for electron microprobe analysis.

REFERENCES

1. C. Mazumdar, R. Nagarajan, C. Godart, L. C. Gupta, M. Latroche, S. K. Dhar, C. Levy-Clement, B. D. Padalia, and R. Vijayaraghavan, *Solid. State Commun.* **87,** 413 (1993).
2. R. Nagarajan, C. Mazumdar, Z. Hossain, S. K. Dhar, K. V. Gopalakrishnan, L. C. Gupta, C. Godart, B. D. Padalia, and R. Vijayaraghavan, *Phys. Rev. Lett.* **72,** 274 (1994).
3. R. J. Cava, H. Takagi, H. W. Zandbergen, J. J. Krajewski, W. F. Peck, T. Siegrist, B. Batlogg, R. B. Van Dover, R. J. Felder, K. Mizuhashi, J. O. Lee, H. Elsaki, and S. Uchida, *Nature* **367,** 252 (1994).
4. T. Siegrist, H. W. Zandbergen, R. J. Cava, J. J. Krajewski, and W. F. Peck, *Nature* **367,** 254 (1994).
5. Various international conferences have sessions on borocarbides: "High T_c superconductivity," Grenoble, France, July 1994; SCES 94, Amsterdam, The Netherlands, August 1994; SCES 95, Goa, India, September 1995; SCES, 96, Zurich, Switzerland, August 1996; MOS, Karlsruhe, Germany, August 1996; ISSB 96, "12th International Symposium on Boron, Borides, and Related Compounds," Baden, Austria, August 1996.
6. H. Eisaki, H. Takagi, R. J. Cava, B. Batlogg, J. J. Krajewski, W. F. Peck, K. Mizuhashi, J. O. Lee, and S. Uchida, *Phys. Rev. B* **50,** 647 (1994).
7. L. C. Gupta, R. Nagarajan, S. K. Dhar, C. Mazumdar, Z. Hossain, C. Godart, C. Levy-Clement, B. D. Padalia, and R. Vijayaraghavan, Bombay "Proceedings of the International Conference on Physical Metallurgy," March 9–11, 1994, p. 494. Gordon and Breach, New York, 1994.
8. C. V. Tomy, G. Balakrishnan, and D. M. K. Paul, *Physica C* **248,** 349 (1995).
9. B. K. Cho, P. C. Canfield, and D. C. Johnston, *Phys. Rev. B* **52,** 3844 (1995).
10. Z. Hossain, L. C. Gupta, R. Nagarajan, S. K. Dhar, C. Godart, and R. Vijayaraghavan, International Conference, SCES 95, Goa, India, September 27–30, 1995. *Physica B* **223** and **224,** 99 (1996).
11. Z. Hossain, S. Dhar, R. Nagarajan, L. C. Gupta, C. Godart, and R. Vijayaraghavan, *IEEE Trans. Magn.* **31,** 4133 (1995).
12. S. K. Dhar, R. Nagarajan, Z. Hossain, E. Tominez, C. Godart, L. C. Gupta, and R. Vijayaraghavan, *Solid State Commun.* **98,** 985 (1996).
13. R. Nagarajan, L. C. Gupta, C. Mazumdar, Z. Hossain, S. K. Dhar, C. Godart, B. D. Padalia, and R. Vijayaraghavan, *J. Alloys and Compounds* **225,** 571 (1994).
14. E. Alleno, Z. Hossain, C. Godart, R. Nagarajan, and L. C. Gupta, *Phys. Rev. B* **52,** 7428 (1995).
15. R. J. Cava, H. Takagi, B. Batlogg, H. W. Zandbergen, J. J. Krajewski, W. F. Peck, R. B. Van Dover, R. J. Felder, T. Siegrist, K. Mizuhashi, J. O. Lee, E. Eisaki, S. A. Carter, and S. Uchida, *Nature* **367,** 146 (1994).
16. Z. Hossain, L. C. Gupta, C. Mazumdar, R. Nagarajan, S. K. Dhar, C. Godart, C. Levy-Clement, B. D. Padalia, and R. Vijayaraghavan, *Solid State Commun.* **92,** 341 (1994).
17. H. C. Ku, C. C. Lai, Y. B. You, J. H. Shieh, and W. Y. Guan, *Phys. Rev. B* **50,** 351 (1994).
18. Z. Hossain, L. C. Gupta, R. Nagarajan, P. Raj, S. K. Dhar, C. Godart, P. Suryanarayana, S. N. Bagchi, V. G. Date, D. S. C. Purushotham, and R. Vijayaraghavan, *Euro Phys. Lett.* **28,** 55 (1994).
19. J. L. Sarrao, M. C. De Andrade, J. Herrmann, S. H. Han, Z. Fisk, M. B. Maple, and R. J. Cava, *Physica C* **229,** 65 (1994).
20. R. J. Cava, B. Batlogg, T. Siegrist, J. J. Krajewski, W. F. Peck, S. Carter, R. J. Felder, H. Takagi, and R. B. Van Dover, *Phys. Rev. B* **49,** 12384 (1994).
21. R. J. Cava, B. Batlogg, J. J. Krajewski, W. F. Peck, T. Siegrist, R. M. Flemeing, S. Carter, H. Takagi, R. J. Felder, R. B. Van Dover, and L. W. Rupp, *Physica C* **226,** 170 (1994).
22. S. A. Carter, B. Batlogg, R. J. Cava, J. J. Krajewski, W. F. Peck, and H. Takagi, *Phys. Rev. B* **50,** 4216 (1994).
23. G. Hilscher, H. Michor, N. M. Hong, T. Holubar, W. Perthold, M. Vybornov, and P. Rogl, *Physica B* **206** and **207,** 542 (1995).
24. H. Michor, T. Holubar, C. Dusek, and G. Hilscher, *Phys. Rev. B* **52,** 16165 (1995).
25. A. K. Gangopadhay and J. S. Schilling, *Preprint Phys. Rev. B* (1996).
26. Q. W. Yan, B. G. Shen, Y. N. Wei, T. Y. Zhao, Y. S. Yao, B. Yin, C. Dong, F. W. Wang, Z. H. Cheng, P. L. Zhang, H. Y. Gong, and Y. F. Li, *Phys. Rev. B* **51,** 8395 (1995).
27. R. J. Cava, H. W. Zandbergen, B. Batlogg, H. Eisaki, H. Takagi, J. J. Krajewski, W. F. Peck, E. M. Gyorgy, and S. Uchida, *Nature* **372,** 245 (1994).
28. H. W. Zandbergen, J. Jansen, R. J. Cava, J. J. Krajewski, and W. F. Peck, *Nature* **372,** 759 (1994).
29. H. Schmidt, M. Weber, and H. F. Braun, *Physica C* **246,** 177 (1995).
30. M. Buchgeister, A. Handstein, J. Klosowski, N. Mattern, P. Verges, and U. Wiesner, *Matter Lett.* **22,** 203 (1995).
31. M. El Massalami and E. M. Baggio-Saitovitch, *J. Magn. Magn. Mat.* **153,** 97 (1996).
32. C. Godart, L. C. Gupta, R. Nagarajan, S. K. Dhar, H. Noel, M. Potel, C. Mazumdar, Z. Hossain, C. Levy-Clement, G. Schiffmacher, B. D. Padalia, R. and R. Vijayaraghavan, *Phys. Rev. B* **51,** 489 (1995).
33. T. Sakai, G. Adachi, and J. Shiokawa, *Solid State Commun.* **40,** 445 (1981).

34. T. Sakai, G. Adachi, and J. Shiokawa, *J. Less Commun. Met*. **84,** 107 (1982).
35. I. Felner, D. Schmitt, B. Barbara, C. Godart, and E. Alleno, "12th International Symposium on Boron, Borides and Related Compounds," Baden, Austria, August, pp. 25–30, 1996.
36. L. C. Gupta, R. Nagarajan, C. Godart, S. K. Dhar, C. Mazumdar, Z. Hossain, C. Levy-Clement, B. D. Padalia, and R. Vijayaraghavan, *Physica C* **235** and **240,** 150 (1994).
37. S. L. Bud'ko, M. Elmassalami, M. B. Fontes, J. Mondragon, W. Vanoni, B. Giordanengo, and E. M. Baggio-Saitovitch, *Physica C* **243,** 183 (1995).
38. A. K. Gangopadhay, A. J. Schuetz, and J. S. Schilling, *Physica C* **246,** 317 (1995).
39. P. Bonville, J. A. Hodges, C. Vaast, E. Alleno, C. Godart, L. C. Gupta, Z. Hossain, and R. Nagarajan, International Conference, SCES 95, Goa, India, September 27–30, 1995. *Physica B* **223** and **224,** 72 (1996).
40. Z. Hossain, S. K. Dhar, K. Elankumaran, R. Nagarajan, L. C. Gupta, C. Godart, R. Vijayaraghavan, "40th Conference on Magnetism and Magnetic Materials," Philadelphia, PA, November 6–9, 1995.
41. D. T. Adroja, B. D. Rainford, A. V. Volkozub, and P. A. J. De Groot, *Physica C* **229,** 193 (1994).
42. H. Fujii, S. Ikeda, T. Kimura, S. Arisawa, K. Hirata, H. Kumakura, K. Kadowaki, and K. Togano, *Jpn. J. Appl. Phys.* **33,** 4B-L590 (1994).
43. S. Ikeda, H. Fujii, T. Kimura, H. Kumakura, K. Kadowaki, and Togano, *Jpn. J. Appl. Phys.* **33,** 7A-3896 (1994).
44. H. W. Zandbergen, W. G. Sloof, R. J. Cava, J. J. Krajewski, and W. F. Peck, *Physica C* **226,** 356 (1994).
45. C. L. Jia, Y. H. Xu, M. Beyss, F. Peter, and K. Urban, *Physica C* **229,** 325 (1994).
46. H. W. Zandbergen, T. J. Gortenmulder, J. L. Sarrac, J. C. Harrison, M. C. De Amdrade, J. Hermann, S. H. Han, Z. Fisk, M. B. Maple, and R. J. Cava, *Physica C* **232,** 328 (1994).
47. Y. Y. Sun, I. Rusakova, R. L. Meng, Y. Cao, P. Gautier-Picard, and C. W. Chu, *Physica C* **230,** 435 (1994).
48. V. Strom, K. S. Kim, A. M. Grishin, and K. V. Rao, *J. Appl. Phys.* **79,** 5860 (1996).
49. V. Strom, K. S. Kim, A. M. Grishin, K. V. Rao, *J. Mater. Res.* **11,** 572 (1996).
50. H. W. Zandbergen, E. J. Van Zwet, J. C. Sarrac, J. C. De Andrade, J. Hermann, S. H. Han, Z. Fisk, M. B. Maple, and R. J. Cava, *Physica C* **229,** 29 (1994).